

## Article

# Early-Life Exposure to Lipopolysaccharide Induces Persistent Changes in Gene Expression Profiles in the Liver and Spleen of Female FVB/N Mice

Elda Dervishi, Dagnachew Hailemariam, Seyed Ali Goldansaz and Burim N. Ametaj \* 

Department of Agricultural Food, and Nutritional Science, University of Alberta,  
Edmonton, AB T6G 2P5, Canada; dervishi@ualberta.ca (E.D.); hailemar@ualberta.ca (D.H.);  
goldansaz@ualberta.ca (S.A.G.)

\* Correspondence: burim.ametaj@ualberta.ca

**Simple Summary:** This study aimed to examine the impact of lipopolysaccharide (LPS) on the gene expression patterns of insulin signaling, innate immunity, and adaptive immunity in the liver and spleen of mice. The findings demonstrate that prolonged and continuous exposure to endotoxemia during early life (at 35 days of age) can initiate molecular mechanisms that result in lasting alterations in gene expression associated with inflammation and adaptive immunity. These changes may contribute to the development of various chronic inflammatory diseases in the liver and spleen. The results indicate that exposing mice to chronic and continuous endotoxemia during early life (at 35 days old) for a duration of 6 weeks can trigger molecular mechanisms that induce lasting changes in gene expression. These changes are associated with inflammation and adaptive immunity and may play a role in the pathobiology of diverse chronic inflammatory diseases affecting the liver and spleen.

**Abstract:** The objective of this study was to investigate how subcutaneous (sc) lipopolysaccharide (LPS) administration affects the gene expression profiles of insulin signaling as well as innate and adaptive immunity genes in mouse livers and spleens. FVB/N female mice were randomly assigned to one of two treatment groups at 5 weeks of age: (1) a six-week subcutaneous injection of saline at 11  $\mu\text{L}/\text{h}$  (control—CON), or (2) a six-week subcutaneous injection of LPS from *Escherichia coli* 0111:B4 at 0.1  $\mu\text{g}/\text{g}$  body weight at 11  $\mu\text{L}/\text{h}$ . At 106 weeks (i.e., 742 days) after the last treatment, mice were euthanized. Following euthanasia, liver and spleen samples were collected, snap frozen, and stored at  $-80^\circ\text{C}$  until gene expression profiling. LPS upregulated nine genes in the liver, according to the findings (*Pparg*, *Frs3*, *Kras*, *Raf1*, *Gsk3b*, *Rras2*, *Hk2*, *Pik3r2*, and *Myd88*). With a 4.18-fold increase over the CON group, *Pparg* was the most up-regulated gene in the liver. Based on the annotation cluster analysis, LPS treatment upregulated liver genes which are involved in pathways associated with hepatic steatosis, B- and T-cell receptor signaling, chemokine signaling, as well as other types of cancers such as endometrial cancer, prostate cancer, and colorectal cancer. LPS increased the spleen expression of *Ccl11*, *Ccl25*, *Il6*, *Cxcl5*, *Pparg*, *Tlr4*, *Nos2*, *Cxcl11*, *Il1a*, *Ccl17*, and *Fcgr3*, all of which are involved in innate and adaptive immune responses and the regulation of cytokine production. Furthermore, functional analysis revealed that cytokine–cytokine receptor interaction and chemokine signaling pathways were the most enriched in LPS-treated mice spleen tissue. Our findings support the notion that early-life LPS exposure can result in long-term changes in gene expression profiling in the liver and spleen tissues of FVB/N female mice.

**Keywords:** mice; LPS; gene expression; liver; spleen



**Citation:** Dervishi, E.; Hailemariam, D.; Goldansaz, S.A.; Ametaj, B.N. Early-Life Exposure to Lipopolysaccharide Induces Persistent Changes in Gene Expression Profiles in the Liver and Spleen of Female FVB/N Mice. *Vet. Sci.* **2023**, *10*, 445. <https://doi.org/10.3390/vetsci10070445>

Academic Editor: Xijun He

Received: 21 May 2023

Revised: 28 June 2023

Accepted: 5 July 2023

Published: 8 July 2023



**Copyright:** © 2023 by the authors. Licensee MDPI, Basel, Switzerland. This article is an open access article distributed under the terms and conditions of the Creative Commons Attribution (CC BY) license (<https://creativecommons.org/licenses/by/4.0/>).

## 1. Introduction

Lipopolysaccharide (LPS), also known as endotoxin, is the major constituent of Gram-negative bacteria's outer membrane, accounting for three-quarters of the outer mem-

brane [1]. Lipopolysaccharide is composed of three components: lipid A, a core polysaccharide, and an O-specific polysaccharide chain [2]. Lipopolysaccharide can enter the host's systemic circulation and cause inflammation when it is released from bacterial membranes during growth, death, or lysis [3]. Many different types of host cells interact with LPS, including antigen-presenting cells like macrophages and dendritic cells [4–6].

Both macrophages and dendritic cells express pattern recognition receptors such as Toll-like receptor 4 (TLR4) to recognize microbial LPS [6,7]. TLR4 activation by LPS results in the release of tumor necrosis factor (TNF), interleukin 1 (IL-1), IL-6, IL-8, and IL-10 [7–10]. Tumor necrosis factor, IL-1, and IL-6 are proinflammatory cytokines that initiate and control local and systemic inflammatory responses, as well as innate and adaptive immune responses. A prolonged immune response to LPS, on the other hand, has serious consequences for specific organs and the host itself. Endotoxemia has been shown to cause systemic inflammation, which has been linked to obesity, diabetes, insulin resistance, and an increased risk of heart disease [11–14]. Endotoxin binding to TLR-4 on vascular endothelial cells has also been proposed to promote atherosclerotic plaque activation [15–17]. Endotoxin has also been shown to increase pancreatic cancer cell invasiveness via the TLR4/MyD88 signaling pathway [18]. Beta-1 integrin-mediated cell adhesion and liver metastasis are also increased by LPS [19].

Furthermore, there is compelling evidence that endotoxin contributes to the onset and progression of alcoholic liver disease (ALD). Endotoxin in the intestinal lumen enters the bloodstream, causing cytokine production from Kupffer cells and initiating the process of liver inflammation, inflammatory cell infiltration, and fibrosis [20,21].

The major mediators of the immune response and systemic inflammatory processes are acute-phase proteins and cytokines produced by liver and spleen [22–24]. Understanding the impact of chronic LPS exposure on gene expression patterns in different immune system organs is therefore critical.

We hypothesized that chronic sc administration of LPS early in life would result in long-term differential gene expression changes in the liver and spleen of FVB/N female mice. As a result, the objectives of this study were to follow selected gene expression profiles in the liver and spleens of FVB/N female mice treated subcutaneously with LPS from *Escherichia coli* 0111:B4 for 6 weeks starting at 5 weeks of age and euthanized 106 weeks later.

## 2. Materials and Methods

### 2.1. Animals and Experimental Design

The Animal Care and Use Committee, Health Sciences, at the University of Alberta approved all methods used during the study in accordance with the Canadian Council on Animal Care [25].

The FVB/N female mice were housed in groups of five per cage, with food and water available at all times and a 12 h light/dark cycle. After one week of acclimatization, five-week-old FVB/N mice ( $n = 5$ ) were randomly assigned to one of two treatment groups: (1) six weeks of saline administration at 11  $\mu\text{L}/\text{h}$ , or (2) six weeks of *Escherichia coli* 0111:B4 LPS injection at 0.1  $\mu\text{g}/\text{g}$  BW at 11  $\mu\text{L}/\text{h}$ .

To avoid the need for repeated injection schedules and frequent animal handling, ALZET<sup>®</sup> osmotic mini pumps (ALZET, Cupertino, CA, USA) were used to administer saline and LPS sc to both groups. ALZET<sup>®</sup> mini-osmotic pumps were inserted subcutaneously (sc) to simulate continuous and minimal oral entry of LPS into the body [26]. During the sc infusion, the manufacturer's recommended procedure was followed. Mice were anesthetized using isoflurane (Baxter Corporation, Mississauga, ON, Canada). Once the mouse became unresponsive to tail pinching, an anesthetic machine was used to administer a low and continuous flow of isoflurane and oxygen (Matrx by Midmark Corporation, Versailles, OH, USA). After shaving and disinfecting a small area on the back of the mouse, a cut was made with sterile surgical scissors. Sutures were used to close the opening after the ALZET<sup>®</sup> mini-osmotic pumps were inserted (ALZET Osmotic Pumps, Cupertino, CA,

USA). The same procedure was repeated after 6 weeks to remove the empty pumps and close the skin opening with sutures [26].

## 2.2. Euthanasia

Five mice ( $n = 5$ ) were euthanized 106 weeks (742 days) after the treatment. Isoflurane (Matrx by Midmark Corporation, Versailles, OH, USA) gas overdose was used to anaesthetize mice [26]. After assessing their reflexes and confirming that they were no longer feeling pain, euthanasia was performed by drawing all of their blood through a cardiac puncture. Following euthanasia, the whole liver and spleen were collected, snap frozen and stored at  $-80\text{ }^{\circ}\text{C}$ . Additionally, beginning with the administration of the treatment at 6 weeks of age, the body weight of each individual mouse in each group was assessed every month.

## 2.3. Total RNA Isolation and First Strand cDNA Synthesis

Following the manufacturer's instructions, total RNA was extracted from liver and spleen tissues ( $n = 3$ ) using the SV total RNA Isolation System (Promega Corporation, Madison, WI, USA). A 30 mg sample was collected for RNA isolation after samples were thawed at room temperature. After that, samples were lysed in an autoclaved tube containing 175  $\mu\text{L}$  of RNA lysis buffer (RLA + BME). Samples were cooked at  $70\text{ }^{\circ}\text{C}$  for 3 min after 350  $\mu\text{L}$  of RNA dilution buffer (RDA) had been added. After that, samples were centrifuged at  $14,000\times g$  for 10 min (model 5430R, Eppendorf, Hamburg, Germany). Two hundred microliters (95%) of ethanol (Commercial Alcohol, Winnipeg, MB, Canada) was added after the clear lysate had been collected into a new 5 mL tube (Promega, Madison, WI, USA). Lysate was cleaned with RNA wash solution after being transferred to the spin basket assembly (Promega, Madison, WI, USA) and centrifuged for 1 min. DNase I was then used to perform on-column DNA digestion in order to eliminate any DNA contamination.

Following additional washing with washing buffers, 100  $\mu\text{L}$  of nuclease-free water was used to elute the total RNA. The purity and concentration of each RNA sample was determined using Nanodrop 8000 instrument (based on measurements at 260 and 280 nm) (peqLab Biotechnologies GmbH, Erlangen, Germany). A cut-off of 1.8 for the A 260/A 280 ratio was employed to assess RNA integrity.

The RT2 miRNA first Strand kit (SABiosciences, Frederick, MD, USA) was used to synthesize cDNA, following the manufacturer's instructions. First, 0.65  $\mu\text{g}$  of total RNA and 2  $\mu\text{L}$  of  $5\times$  gDNA elimination buffer were combined to create the first genomic DNA elimination mix. The final volume was adjusted to 10 mL by adding ddH<sub>2</sub>O. The mixture was gently stirred using a pipette (Eppendorf, Hamburg, Germany), briefly centrifuged (Eppendorf, Hamburg, Germany), and incubated at  $42\text{ }^{\circ}\text{C}$  for 5 min. Thereafter, a 10  $\mu\text{L}$  RT cocktail was made for each sample by mixing 4  $\mu\text{L}$  of  $5\times$  RT buffer 3 (BC3), 1  $\mu\text{L}$  of primer and external control mix (P2), 2  $\mu\text{L}$  of RT enzyme mix 3 (RE3), and 3  $\mu\text{L}$  of ddH<sub>2</sub>O. Then, 10  $\mu\text{L}$  of the RT cocktail was added to 10  $\mu\text{L}$  of each of the genomic DNA removal mixtures. The mixture was gently blended using a pipettor, then incubated at  $42\text{ }^{\circ}\text{C}$  for 15 min. The reaction was stopped by heating the mixture to  $95\text{ }^{\circ}\text{C}$  for 5 min. Each 20  $\mu\text{L}$  cDNA synthesis reaction was then administered 91  $\mu\text{L}$  of ddH<sub>2</sub>O and stored at  $-20\text{ }^{\circ}\text{C}$  until analysis.

## 2.4. Quantitative PCR (qPCR) Assay

The gene expression profiling in liver and spleen tissues was determined using qPCR on a StepOnePlus ABI Prism platform (Applied Biosystems, Burlington, ON, Canada). To assess gene expression in the liver, the Mice Insulin Signaling Pathway Kit and the Innate and Adaptive Immunity PCR Array Kit were used (Qiagen, Mississauga, ON, Canada). The Insulin Signaling Pathway Kit examines 84 genes that are involved in cell growth and differentiation, transcription factors, glucose, lipid, and protein metabolism, insulin receptor-associated proteins, and the PI-3 kinase and MAPK pathways. The Innate and Adaptive Immunity kit detects 84 genes associated with IL-1R/TLR members, host defense

against bacteria, innate immune response, and septic shock genes. Both PCR array kits included specific primers for 84 genes, a control for genomic DNA contamination (GDC), a control for reverse transcription (RTC), and a positive PCR control. At the end stage, spleen samples were collected, and gene expression was evaluated using a RT2 PCR array. The 96-well custom RT2-PCR array was used to quantify 84 inflammation-related genes, 5 housekeeping genes (B2M, Actb, Gapdh, Gusb, and HSP90ab1), 3 reverse transcription controls (RTC), 3 positive PCR controls, and mouse genomic DNA contamination controls. An Excel spreadsheet containing the mouse gene symbol and ResSeq number was sent to SABioscience for manufacturing (SABiosciences, Frederick, MD, USA).

Prior to real-time PCR profiling, each of the 20  $\mu$ L first strand cDNA products from all biological replicates from the treatment and negative control groups received 91  $\mu$ L of DNase/RNase-free water. Then, 102  $\mu$ L of diluted cDNA template, 1350  $\mu$ L of RT2 SYBR Green PCR master mix, and 1248  $\mu$ L of DNase/RNase-free water were combined to create a PCR master mix. Twenty-five microliters of this mixture was added to each well of the 96-well plate, which contained sequence-specific primer sets for each gene and their respective controls. After a brief centrifugation (Eppendorf, Hamburg, Germany), the plate was loaded onto the StepOnePlus Real-Time PCR System (Applied Biosystems, Darmstadt, Germany) and run with a thermal program of initial heating at 95 °C for 10 min, followed by 40 cycles of 95 °C for 15 s and 60 °C for 1 min. A melting curve generated at the end of the PCR protocol was used to control the specificity of the amplification.

### 2.5. Statistical Analysis

The  $\Delta\Delta$ CT method from the PCR array data analysis web portal "<http://www.sabiosciences.com/pcrarraydataanalysis.php> (accessed on 14 October 2015)" was used to analyze the fold change in the mRNA expression of selected genes included in the custom PCR array. For each gene in the custom PCR array, the software calculated the average threshold cycle values for biological replicates from both the treatment and control groups. All genes with a ct value greater than 35 and those that were undetected were excluded from the analysis. The data were normalized by adjusting all comparative threshold (ct) values for the average ct value of the array's endogenous controls [26].

Gene expression data were analyzed with t-tests and treatment was included as a fixed factor. Fold change values greater than 1.5 and  $p \leq 0.05$  were used as cut-off values to identify genes that were differentially expressed in the treatment groups versus the saline-treated negative control group. MetaboAnalyst "<https://www.metaboanalyst.ca> (accessed on 25 April 2023)" was used to perform cluster analysis for gene expression [27]. Each sample began as a separate cluster in hierarchical cluster analysis, and the algorithm proceeded to combine them until all samples belong to one cluster. When performing hierarchical clustering, two parameters were considered—the first was a similarity measure, and the second was a clustering algorithm. The Euclidian and Ward clustering algorithms were used to measure distance [27].

The Functional Annotation Cluster (FAC) tool based on the Gene Ontology (GO) annotation function was used to determine pathways and processes of major biological significance and importance using the Database for Annotation, Visualization, and Integrated Discovery (DAVID; <https://david.ncifcrf.gov/tools.jsp> (accessed on 25 April 2023)) v6.7b [28]. The gene lists obtained after statistical analysis were subjected to a DAVID FAC analysis. The medium stringency EASE score parameters were selected to show confident enrichment scores of functional significance and importance of the investigated pathways and processes. As a threshold for cluster significance, an enrichment score of 1.3 was used [29]. In addition, the ClueGo plug-in and Cytoscape program [30,31] were used visualize the differentially expressed genes in the liver and spleen of mice according to the pathways in which they are involved. We used the *Mus musculus* database and KEGG pathways to develop a pathway network [30].

### 3. Results

#### 3.1. Weight and Gene Expression Profiling in the Liver and Spleen Tissues

Overall, the treatment did not have a significant effect on the weight of the mice ( $p = 0.45$ ). However, there was a significant effect observed for the week factor ( $p < 0.001$ ), indicating that the age of the mice had a notable influence. This is further illustrated in Figure S1. The results of gene expression profiles in the liver and spleen are shown in Tables 1 and 2, respectively. A total of seven genes were significantly differentially expressed in the liver of mice that received subcutaneous administration of LPS. Six genes (*Pparg*, *Frs3*, *Kras*, *Raf1*, *Gsk3b*, and *Rras2*) were up-regulated in the liver. The most up-regulated gene in the liver tissue was *Pparg*, with a 4.18-fold increase compared to the CON group. In addition, there were tendencies for overexpression of *Hk2* ( $p = 0.08$ ), *Pik3r2* ( $p = 0.06$ ), *Myd88* ( $p = 0.07$ ), and *Nfkbia* ( $p = 0.07$ ) in the LPS group. In addition, *Cxcl10* was significantly down-regulated, decreasing by 3.6-fold compared to the CON group. Other genes like *Ptprf*, *Acaca*, *Ccr5*, *Irf3*, *Irf7*, *Lyz2*, *Mbl2*, and *Stat1* tended to be down-regulated (see Table 1 for  $p$  values).

**Table 1.** List of differentially regulated genes in the LPS-treated group in the liver.

Gene Symbol	Description of the Genes	Fold-Change	$p$ -Value
<b>Up-Regulated DE Genes in LPS vs. Saline</b>			
<i>Pparg</i>	Peroxisome proliferator activated receptor gamma	4.18	0.02
<i>Frs3</i>	Fibroblast growth factor receptor substrate 3	2.65	0.0005
<i>Kras</i>	V-Ki-ras2 Kirsten rat sarcoma viral oncogene homolog	2.08	0.0008
<i>Raf1</i>	V-raf-leukemia viral oncogene 1	1.66	0.006
<i>Gsk3b</i>	Glycogen synthase kinase 3 beta	1.66	0.007
<i>Rras2</i>	Related RAS viral (r-ras) oncogene homolog 2	1.65	0.007
<i>Hk2</i>	Hexokinase 2	2.09	0.08
<i>Pik3r2</i>	Phosphatidylinositol 3-kinase, regulatory subunit, polypeptide 2 (p85 beta)	2.05	0.06
<b>Down-Regulated DE genes in LPS vs. Saline</b>			
<i>Cxcl10</i>	Chemokine (C-X-C motif) ligand 10	−3.57	0.01
<i>Ptprf</i>	Protein tyrosine phosphatase, receptor type, F	−2.41	0.07
<i>Acaca</i>	Acetyl-Coenzyme A carboxylase alpha	−2.41	0.08
<i>Ccr5</i>	Chemokine (C-C motif) receptor 5	−2.2	0.06
<i>Irf3</i>	Interferon regulatory factor 3	−1.7	0.06
<i>Irf7</i>	Interferon regulatory factor 7	−1.7	0.06
<i>Lyz2</i>	Lysozyme 2	−2.2	0.06
<i>Mbl2</i>	Mannose-binding lectin (protein C) 2	−1.7	0.06
<i>Stat1</i>	Signal transducer and activator of transcription 1	−3.5	0.08

The results also showed that LPS in the spleen significantly altered the expression of 22 genes ( $p < 0.05$ ). Twelve genes were up-regulated (*Ccl25*, *Il6*, *Ccl17*, *Pparg*, *Ccl11*, *Prnd*, *Cxcl5*, *Il1a*, *Cxcl11*, *Nos2*, *Tlr4*, and *Fcgr3*) and ten genes (*Fyn*, *Grn*, *Lyz2*, *H2-k1*, *Fcgr2b*, *Egr1*, *Notch1*, *Rtp4*, *Ifi27i2a*, and *Ache*) were down-regulated ( $p < 0.05$ ). In addition, there were tendencies for the down-regulation of *Apoe* ( $p = 0.06$ ), *Gbp4* ( $p = 0.07$ ), and *Atp1b1* ( $p = 0.08$ ) in the spleen (Table 2). The most up-regulated gene in the spleen was *Fcgr3* (Fc fragment of Ig, low affinity IIb, receptor) with a 18.23-fold increase compared to the CON group of mice. *Lyz2* (Lysozyme 2) and *Ifi27i2a* (interferon, alpha-inducible protein 27 like 2A) were the most down-regulated genes, with −11.2- and −8.94-fold changes, respectively, in the LPS-treated group compared to the control (Table 2).

Two genes, *Pparg* and *Lyz2*, were differentially expressed in both the liver and spleen. Both organs exhibited an increased expression for *Pparg* and a decrease in the expression of *Lyz2*. A heatmap of gene expression of the control and LPS group in the liver and spleen is shown in Figure 1a,b, respectively.

**Table 2.** List of differentially regulated genes in the LPS-treated group in the spleen.

Gene Symbol	Description of the Gene	Fold-Change	p-Value
<b>Up-Regulated DE Genes in LPS vs. Saline</b>			
<i>Ccl25</i>	Chemokine (C-C motif) ligand 25	2.27	0.0002
<i>Il6</i>	Interleukin 6	2.89	0.0007
<i>Ccl17</i>	Chemokine (C-C motif) ligand 17	1.78	0.0009
<i>Pparg</i>	Peroxisome proliferating receptor gamma	5.81	0.001
<i>Ccl11</i>	Chemokine (C-C) ligand 11	2.29	0.001
<i>Prnd</i>	Prion protein 2 (dublet)	2.9	0.002
<i>Cxcl5</i>	Chemokine (C-X-C motif) ligand 5	1.77	0.006
<i>Il1a</i>	Interleukin 1a	1.8	0.011
<i>Cxcl11</i>	Chemokine (C-X-C motif) ligand 11	2.83	0.025
<i>Nos2</i>	Nitric oxide synthase 2	1.11	0.035
<i>Tlr4</i>	Toll like receptor 4	1.43	0.039
<i>Fcgr3</i>	Fc fragment of Ig, low affinity IIb, receptor	18.23	0.045
<b>Down-Regulated DE genes in LPS vs. Saline</b>			
<i>Fyn</i>	Fyn oncogene related to SRC, FGR YES	-4.41	0.002
<i>Grn</i>	Granulin	-2.19	0.003
<i>Lyz2</i>	Lysozyme 2	-11.02	0.005
<i>H2-k1</i>	Histocompatibility 2, K1, K region; similar to H-2K(d) antigen	-4.38	0.003
<i>Fcgr2b</i>	Fc receptor, IgG, low affinity IIb	-4.4	0.006
<i>Egr1</i>	Early growth response 1	-2.2	0.009
<i>Notch1</i>	Notch1	-2.21	0.010
<i>Rtp4</i>	Receptor (chemosensory) transporter protein4	-1.41	0.014
<i>Ifi27i2a</i>	Interferon, alpha-inducible protein 27 like 2A	-8.94	0.016
<i>Ache</i>	Acetylcholinesterase	-1.1	0.019
<i>ApoE</i>	Apolipoprotein E	-1.09	0.065
<i>Gbp4</i>	Guanylate binding protein 4	-2.2	0.072
<i>Atp1b1</i>	ATPase, Na <sup>+</sup> /K <sup>+</sup> transporting, beta 1 polypeptide	-2.74	0.090

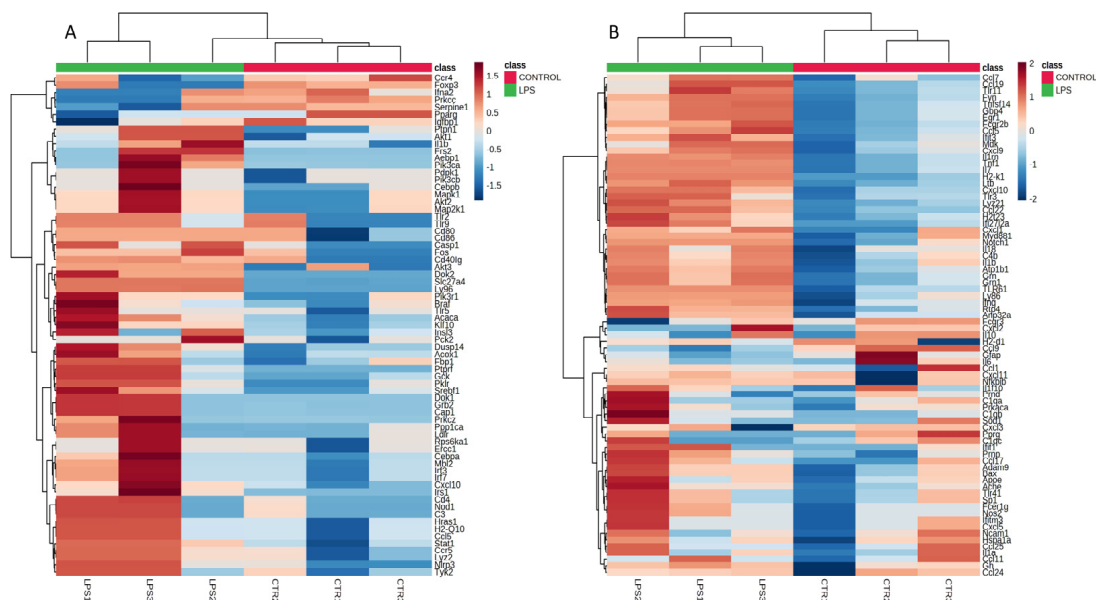


**Figure 1.** Hierarchical cluster analysis of gene expression in mouse (A) livers and (B) spleens.

### 3.2. Functional Annotation Analysis

The results of DAVID functional annotation clustering (FAC) of differentially expressed genes in the liver tissue showed that the most enriched pathway clusters, with an enrichment score of 2.67, was ‘hepatitis C, followed by ‘chemokine signaling pathway’,

‘endometrial cancer’, ‘prolactin signaling pathway’, ‘EGFR tyrosine kinase inhibitor resistance’, and ‘B-cell receptor signaling pathway’. This pathway involved the genes *Kras*, *Gsk3b*, *Raf1*, *Nfkbia*, and *Pik3r2* (Table 3). In addition, several disease pathways including the ‘endometrial cancer’, ‘colorectal cancer’, ‘ErbB signaling’, ‘breast cancer’, and ‘gastric cancer’ pathways with *Kras*, *Gsk3b*, and *Raf1* genes were significantly enriched (Table 3).

**Table 3.** Enriched pathway clusters determined by DAVID functional annotation clustering of up-regulated and down-regulated DE genes in CTR vs. LPS in mice liver.

Annotation Cluster 1: Enrichment Score: 2.67					
Category	Term	Genes	Count	p-Value	Benjamini
KEGG_PATHWAY	Hepatitis C	<i>Kras, Cxcl10, Gsk3b, Raf1</i>	4	$5.90 \times 10^{-5}$	$5.60 \times 10^{-3}$
KEGG_PATHWAY	Chemokine signaling pathway	<i>Kras, Cxcl10, Gsk3b, Raf1</i>	4	$9.20 \times 10^{-5}$	$5.60 \times 10^{-3}$
GOTERM_BP_DIRECT	Signal transduction	<i>Kras, Gsk3b, Pparg, Rras2, Raf1</i>	5	$3.10 \times 10^{-4}$	$1.00 \times 10^{-1}$
KEGG_PATHWAY	Endometrial cancer	<i>Kras, Gsk3b, Raf1</i>	3	$4.00 \times 10^{-4}$	$1.40 \times 10^{-2}$
KEGG_PATHWAY	Prolactin signaling pathway	<i>Kras, Gsk3b, Raf1</i>	3	$6.50 \times 10^{-4}$	$1.40 \times 10^{-2}$
KEGG_PATHWAY	EGFR tyrosine kinase inhibitor resistance	<i>Kras, Gsk3b, Raf1</i>	3	$7.50 \times 10^{-4}$	$1.40 \times 10^{-2}$
KEGG_PATHWAY	B-cell receptor signaling pathway	<i>Kras, Gsk3b, Raf1</i>	3	$7.80 \times 10^{-4}$	$1.40 \times 10^{-2}$
KEGG_PATHWAY	ErbB signaling pathway	<i>Kras, Gsk3b, Raf1</i>	3	$8.40 \times 10^{-4}$	$1.40 \times 10^{-2}$
KEGG_PATHWAY	Colorectal cancer	<i>Kras, Gsk3b, Raf1</i>	3	$9.30 \times 10^{-4}$	$1.40 \times 10^{-2}$
KEGG_PATHWAY	Prostate cancer	<i>Kras, Gsk3b, Raf1</i>	3	$1.20 \times 10^{-3}$	$1.40 \times 10^{-2}$
KEGG_PATHWAY	Melanogenesis	<i>Kras, Gsk3b, Raf1</i>	3	$1.20 \times 10^{-3}$	$1.40 \times 10^{-2}$
KEGG_PATHWAY	T cell receptor signaling pathway	<i>Kras, Gsk3b, Raf1</i>	3	$1.30 \times 10^{-3}$	$1.40 \times 10^{-2}$
KEGG_PATHWAY	Growth hormone synthesis, secretion and action	<i>Kras, Gsk3b, Raf1</i>	3	$1.60 \times 10^{-3}$	$1.40 \times 10^{-2}$
KEGG_PATHWAY	Thyroid hormone signaling pathway	<i>Kras, Gsk3b, Raf1</i>	3	$1.70 \times 10^{-3}$	$1.40 \times 10^{-2}$
KEGG_PATHWAY	Neurotrophin signaling pathway	<i>Kras, Gsk3b, Raf1</i>	3	$1.70 \times 10^{-3}$	$1.40 \times 10^{-2}$
KEGG_PATHWAY	Pathways in cancer	<i>Kras, Gsk3b, Pparg, Raf1</i>	4	$2.00 \times 10^{-3}$	$1.40 \times 10^{-2}$
KEGG_PATHWAY	Insulin signaling pathway	<i>Kras, Gsk3b, Raf1</i>	3	$2.30 \times 10^{-3}$	$1.40 \times 10^{-2}$
KEGG_PATHWAY	Signaling pathways regulating pluripotency of stem cells	<i>Kras, Gsk3b, Raf1</i>	3	$2.30 \times 10^{-3}$	$1.40 \times 10^{-2}$
KEGG_PATHWAY	Breast cancer	<i>Kras, Gsk3b, Raf1</i>	3	$2.60 \times 10^{-3}$	$1.40 \times 10^{-2}$
KEGG_PATHWAY	Gastric cancer	<i>Kras, Gsk3b, Raf1</i>	3	$2.70 \times 10^{-3}$	$1.40 \times 10^{-2}$
KEGG_PATHWAY	mTOR signaling pathway	<i>Kras, Gsk3b, Raf1</i>	3	$2.90 \times 10^{-3}$	$1.50 \times 10^{-2}$
KEGG_PATHWAY	Hepatocellular carcinoma	<i>Kras, Gsk3b, Raf1</i>	3	$3.60 \times 10^{-3}$	$1.70 \times 10^{-2}$
KEGG_PATHWAY	Axon guidance	<i>Kras, Gsk3b, Raf1</i>	3	$3.90 \times 10^{-3}$	$1.80 \times 10^{-2}$
KEGG_PATHWAY	Kaposi sarcoma-associated herpesvirus infection	<i>Kras, Gsk3b, Raf1</i>	3	$5.90 \times 10^{-3}$	$2.40 \times 10^{-2}$
KEGG_PATHWAY	Human cytomegalovirus infection	<i>Kras, Gsk3b, Raf1</i>	3	$7.60 \times 10^{-3}$	$2.80 \times 10^{-2}$
GOTERM_MF_DIRECT	nucleotide binding	<i>Kras, Gsk3b, Rras2, Raf1</i>	4	$1.30 \times 10^{-2}$	$5.10 \times 10^{-1}$
KEGG_PATHWAY	PI3K-Akt signaling pathway	<i>Kras, Gsk3b, Raf1</i>	3	$1.50 \times 10^{-2}$	$5.00 \times 10^{-2}$
KEGG_PATHWAY	Human papillomavirus infection	<i>Kras, Gsk3b, Raf1</i>	3	$1.50 \times 10^{-2}$	$5.00 \times 10^{-2}$
KEGG_PATHWAY	Alzheimer’s disease	<i>Kras, Gsk3b, Raf1</i>	3	$1.70 \times 10^{-2}$	$5.50 \times 10^{-2}$
KEGG_PATHWAY	Pathways of neurodegeneration—multiple diseases	<i>Kras, Gsk3b, Raf1</i>	3	$2.50 \times 10^{-2}$	$7.50 \times 10^{-2}$
GOTERM_MF_DIRECT	protein binding	<i>Kras, Gsk3b, Pparg, Rras2, Raf1</i>	5	$6.30 \times 10^{-2}$	$8.70 \times 10^{-1}$

Category: original database/resource where the terms originate; Term: enriched terms associated with our gene list; Count: genes involved in the term; p-value: Benjamini adjusted p-value. GOTERM: Gene Ontology Term; BP: biological process; MF: molecular function.

The results of FAC of differentially expressed genes in the spleen revealed that the most enriched pathway cluster had an enrichment score of 4.25, followed by a second cluster with a score of 3.07. The top five enriched biological processes were the ‘inflammatory response’ with 10 genes (*Ccl11, Ccl17, Ccl25, Cxcl11, Cxcl5, Il1a, Il6, Nos2, Pparg, Tlr4*), ‘neutrophil chemotaxis’ with 6 genes (*Fgr, Ccl11, Ccl17, Ccl25, Cxcl11, Cxcl5*), ‘positive regulation of ERK1 and ERK2 cascade’ with 7 genes (*Ccl11, Ccl17, Ccl25, Il1a, Il6, Notch1, Tlr4*), ‘cytokine activity’ with 7 genes (*Ccl11, Ccl17, Ccl25, Cxcl5, Grn, Il1a, Il6*) and ‘chemokine activity’ with 5 genes (*Ccl11, Ccl17, Ccl25, Cxcl11, Cxcl5*; Table 4). In addition, the results of DAVID FAC showed that ‘viral protein interaction with cytokine and cytokine receptor’ with six genes (*Ccl11, Ccl17, Ccl25, Cxcl11, Cxcl5, Il6*), ‘chemokine receptors bind chemokines’ with five genes (*Ccl11, Ccl17, Ccl25, Cxcl11, Cxcl5*), and ‘cytokine-cytokine receptor interaction’ with seven genes (*Ccl11, Ccl17, Ccl25, Cxcl11, Cxcl5, Il1a, Il6*) were the most enriched pathways in the spleen tissue in the LPS-treated mice (Table 4).

**Table 4.** Most enriched pathway clusters as determined by DAVID functional annotation clustering of up-regulated and down-regulated DE genes in CTR vs. LPS in mouse spleens.

Annotation Cluster 1: Enrichment Score: 4.25					
Category	Term	Genes	Count	p-Value	Benjamini
GOTERM_BP_DIRECT	Inflammatory response	<i>Ccl11, Ccl17, Ccl25, Cxcl11, Cxcl5, Il1a, Il6, Nos2, Pparg, Tlr4</i>	10	$5.80 \times 10^{-11}$	$4.20 \times 10^{-8}$
GOTERM_BP_DIRECT	Neutrophil chemotaxis	<i>Fgr, Ccl11, Ccl17, Ccl25, Cxcl11, Cxcl5</i>	6	$1.40 \times 10^{-8}$	$5.20 \times 10^{-6}$
GOTERM_BP_DIRECT	positive regulation of ERK1 and ERK2 cascade	<i>Ccl11, Ccl17, Ccl25, Il1a, Il6, Notch1, Tlr4</i>	7	$9.50 \times 10^{-8}$	$2.30 \times 10^{-5}$
GOTERM_MF_DIRECT	Cytokine activity	<i>Ccl11, Ccl17, Ccl25, Cxcl5, Grn, Il1a, Il6</i>	7	$1.30 \times 10^{-7}$	$9.30 \times 10^{-6}$
GOTERM_MF_DIRECT	Chemokine activity	<i>Ccl11, Ccl17, Ccl25, Cxcl11, Cxcl5</i>	5	$1.30 \times 10^{-7}$	$9.30 \times 10^{-6}$
GOTERM_BP_DIRECT	Chemokine-mediated signaling pathway	<i>Ccl11, Ccl17, Ccl25, Cxcl11, Cxcl5</i>	5	$2.20 \times 10^{-7}$	$4.10 \times 10^{-5}$
GOTERM_BP_DIRECT	Immune response	<i>Ccl11, Ccl25, Cxcl11, Cxcl5, Il1a, H2-k1, Tlr4</i>	8	$3.20 \times 10^{-7}$	$4.60 \times 10^{-4}$
KEGG_PATHWAY	Viral protein interaction with cytokine and cytokine receptor	<i>Ccl11, Ccl17, Ccl25, Cxcl11, Cxcl5, Il6</i>	6	$6.60 \times 10^{-7}$	$7.30 \times 10^{-4}$
REACTOME_PATHWAY	Chemokine receptors bind chemokines	<i>Ccl11, Ccl17, Ccl25, Cxcl11, Cxcl5</i>	5	$2.40 \times 10^{-6}$	$3.30 \times 10^{-4}$
GOTERM_BP_DIRECT	Cellular response to interferon-gamma	<i>Ccl11, Ccl17, Ccl25, Nos2, Tlr4</i>	5	$4.10 \times 10^{-6}$	$4.90 \times 10^{-4}$
GOTERM_BP_DIRECT	Chemotaxis	<i>Ccl11, Ccl17, Ccl25, Cxcl11, Cxcl5</i>	5	$9.10 \times 10^{-6}$	$8.30 \times 10^{-4}$
KEGG_PATHWAY	Cytokine–cytokine receptor interaction	<i>Ccl11, Ccl17, Ccl25, Cxcl11, Cxcl5, Il1a, Il6</i>	7	$1.00 \times 10^{-5}$	$4.00 \times 10^{-4}$
GOTERM_BP_DIRECT	Antimicrobial humoral immune response mediated by antimicrobial peptide	<i>Ccl11, Ccl17, Ccl25, Cxcl11, Cxcl5</i>	5	$1.10 \times 10^{-5}$	$8.50 \times 10^{-4}$
GOTERM_BP_DIRECT	Killing of cells of other organisms	<i>Ccl11, Ccl17, Ccl25, Lyz2</i>	4	$1.90 \times 10^{-5}$	$1.40 \times 10^{-3}$
GOTERM_BP_DIRECT	Cellular response to interleukin-1	<i>Ccl11, Ccl17, Ccl25, Il6</i>	4	$7.20 \times 10^{-5}$	$4.80 \times 10^{-3}$
REACTOME_PATHWAY	Peptide ligand-binding receptors	<i>Ccl11, Ccl17, Ccl25, Cxcl11, Cxcl5</i>	5	$3.20 \times 10^{-5}$	$2.10 \times 10^{-2}$
GOTERM_MF_DIRECT	CCR chemokine receptor binding	<i>Ccl11, Ccl17, Ccl25</i>	3	$3.50 \times 10^{-4}$	$1.70 \times 10^{-2}$
KEGG_PATHWAY	Chemokine signaling pathway	<i>Ccl11, Ccl17, Ccl25, Cxcl11, Cxcl5</i>	5	$3.80 \times 10^{-4}$	$6.10 \times 10^{-2}$

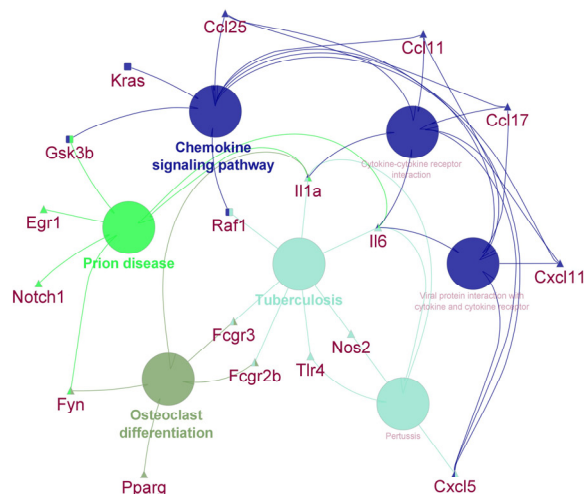


Table 4. Cont.

Annotation Cluster 1: Enrichment Score: 4.25					
Category	Term	Genes	Count	p-Value	Benjamini
GOTERM_BP_DIRECT	Cellular response to tumor necrosis factor	<i>Ccl11, Ccl17, Ccl25, Il6</i>	4	$4.00 \times 10^{-4}$	$1.60 \times 10^{-2}$
GOTERM_BP_DIRECT	Lymphocyte chemotaxis	<i>Ccl11, Ccl17, Ccl25</i>	3	$4.10 \times 10^{-4}$	$1.60 \times 10^{-2}$
GOTERM_BP_DIRECT	Monocyte chemotaxis	<i>Ccl11, Ccl17, Ccl25</i>	3	$6.20 \times 10^{-4}$	$2.20 \times 10^{-2}$
KEGG_PATHWAY	IL-17 signaling pathway	<i>Ccl11, Ccl17, Ccl25, Il6</i>	4	$6.50 \times 10^{-4}$	$8.10 \times 10^{-3}$
REACTOME_PATHWAY	Class A/1 (Rhodopsin-like receptors)	<i>Ccl11, Ccl17, Ccl25, Cxcl11, Cxcl5</i>	5	$2.10 \times 10^{-3}$	$9.30 \times 10^{-2}$
GOTERM_BP_DIRECT	Cell chemotaxis	<i>Ccl17, Ccl25, Cxcl11</i>	3	$3.50 \times 10^{-3}$	$7.50 \times 10^{-2}$
REACTOME_PATHWAY	GPCR ligand binding	<i>Ccl11, Ccl17, Ccl25, Cxcl11, Cxcl5</i>	5	$5.20 \times 10^{-3}$	$1.20 \times 10^{-1}$
REACTOME_PATHWAY	G alpha (i) signaling events	<i>Ccl11, Ccl25, Cxcl11, Cxcl5</i>	4	$1.30 \times 10^{-2}$	$2.50 \times 10^{-1}$
GOTERM_BP_DIRECT	Positive regulation of GTPase activity	<i>Ccl11, Ccl17, Ccl25</i>	3	$1.60 \times 10^{-2}$	$2.20 \times 10^{-1}$
REACTOME_PATHWAY	Signaling by GPCR	<i>Ccl11, Ccl17, Ccl25, Cxcl11, Cxcl5</i>	5	$2.20 \times 10^{-2}$	$3.60 \times 10^{-1}$
REACTOME_PATHWAY	Signal transduction	<i>Fyn, Ccl11, Ccl17, Ccl25, Cxcl11, Cxcl5, Il6, Notch1</i>	8	$8.20 \times 10^{-2}$	$8.90 \times 10^{-1}$
REACTOME_PATHWAY	GPCR downstream signaling	<i>Ccl11, Ccl25, Cxcl11, Cxcl5</i>	4	$8.50 \times 10^{-2}$	$8.90 \times 10^{-1}$
GOTERM_BP_DIRECT	G-protein coupled receptor signaling pathway	<i>Ccl11, Ccl17, Ccl25</i>	3	$5.20 \times 10^{-1}$	$1.00 \times 10^{-1}$
Annotation Cluster 2: Enrichment Score: 3.07					
GOTERM_BP_DIRECT	Cellular response to lipopolysaccharide	<i>Cxcl11, Cxcl5, Il1a, Il6, Nos2, Tlr4</i>	6	$8.90 \times 10^{-6}$	$8.30 \times 10^{-4}$
KEGG_PATHWAY	Pertussis	<i>Cxcl5, Il1a, Il6, Nos2, Tlr4</i>	5	$1.10 \times 10^{-5}$	$4.00 \times 10^{-4}$
KEGG_PATHWAY	Tuberculosis	<i>Fcgr3, Fcgr2b, Il1a, Nos2, Tlr4</i>	6	$1.50 \times 10^{-5}$	$4.30 \times 10^{-4}$
GOTERM_BP_DIRECT	Positive regulation of interleukin-6 production	<i>Il1a, Il6, Nos2, Tlr4</i>	4	$1.80 \times 10^{-4}$	$1.00 \times 10^{-2}$
GOTERM_BP_DIRECT	Positive regulation of apoptotic process	<i>Il6, Nos2, Notch1, Pparg, Tlr4</i>	5	$5.00 \times 10^{-4}$	$1.80 \times 10^{-2}$
GOTERM_BP_DIRECT	Positive regulation of interleukin-8 production	<i>Il6, Nos2, Tlr4</i>	3	$1.60 \times 10^{-3}$	$3.90 \times 10^{-2}$
GOTERM_BP_DIRECT	Signal transduction	<i>Ccl17, Cxcl11, Il6, Nos2, Pparg, Tlr4</i>	6	$1.00 \times 10^{-2}$	$1.60 \times 10^{-1}$
KEGG_PATHWAY	Toll-like receptor signaling pathway	<i>Cxcl11, Il6, Tlr4</i>	3	$1.50 \times 10^{-2}$	$1.00 \times 10^{-1}$
KEGG_PATHWAY	Chagas disease	<i>Il6, Nos2, Tlr4</i>	3	$1.60 \times 10^{-2}$	$1.00 \times 10^{-1}$
KEGG_PATHWAY	Amoebiasis	<i>Il6, Nos2, Tlr4</i>	3	$1.70 \times 10^{-2}$	$1.10 \times 10^{-1}$
KEGG_PATHWAY	HIF-1 signaling pathway	<i>Il6, Nos2, Tlr4</i>	3	$1.90 \times 10^{-2}$	$1.10 \times 10^{-1}$

Category: original database/resource where the terms origin; Term: enriched terms associated with our gene list; Count: genes involved in the term; p-value: Benjamini adjusted p-value GOTERM: Gene Ontology Term; BP: biological process; MF: molecular function.

A visualization of the differentially expressed genes in the liver and spleen of mice according to the pathways in which they are involved is shown in Figure 2. The chemokine signaling pathway, cytokine–cytokine receptor interaction and viral protein interaction with cytokines and cytokine receptors were significantly enriched. Furthermore, the differentially expressed genes participate in prion disease and tuberculosis.



**Figure 2.** Gene network of differentially expressed genes in the liver and spleen of mice treated with subcutaneous LPS. Genes that are differentially expressed in the liver are represented by a rectangle shape and genes that are differentially expressed in the spleen are represented by a triangle shape. Functionally grouped networks with terms as nodes are linked based on their kappa score level (0.4).

#### 4. Discussion

LPS injected into the bloodstream or intraperitoneally has been shown to be removed from circulation by monocytes, macrophages, and neutrophils in the systemic circulation, as well as resident macrophages in the liver and spleen [32]. The liver contains nearly 80% of all resident macrophages in the body, making it a critical organ for removing and detoxifying pathogen-borne antigens such as LPS [33].

In a related paper, we showed that early-life subcutaneous LPS administration in the same mice resulted in long-term changes in gene expression profiling in the brain 106 weeks later [26]. In this study, we hypothesized that 6 weeks of subcutaneous LPS administration at the age of 35 days would result in long-term changes in the gene expression profiles in the liver and spleen of mice 106 weeks after treatment.

Indeed, we discovered that mice exposed to LPS at a young age displayed long-term changes in their gene expression profiles in both the liver and spleen. One hundred and six weeks after LPS administration, eight genes (*Pparg*, *Frs3*, *Kras*, *Raf1*, *Gsk3b*, *Rras2*, *Hk2*, and *Pik3r2*) were up-regulated in the livers of mice. When compared to the control group, *Pparg* was the most up-regulated gene in the liver, with a 4.18-fold increase. PPARG binds to compounds that promote the proliferation of peroxisomes, which are liver organelles that aid in the oxidation of fatty acids. Furthermore, *Pparg* regulates energy metabolism, adipocyte differentiation, glucose homeostasis, and the promotion of lipid storage, inducing fatty liver [34]. PPARG, as an anti-inflammatory protein, is important in regulating immune responses during inflammation [35–37]. In another study, LPS was shown to downregulate *Pparg* expression in macrophages and in the liver of rats during sepsis via an increase in TNF release [38,39]. The difference can be explained by the fact that the authors of that study measured *Pparg* expression in an animal sepsis model 10 h after administering a single higher dose of LPS. However, in our study, we looked at the long-term effects of a low dose of LPS administered chronically and continuously on *Pparg* expression.

Intriguingly, genes related to TLR and the immune response pathway were down-regulated in the liver in our study. Because the *Pparg* product is an anti-inflammatory protein, its up-regulation may have contributed to the down-regulation of pro-inflammatory responses in the liver. It is hypothesized that the up-regulation of *Pparg* may have suppressed the activation of liver-resident macrophages (i.e., Kupffer cells) by down-regulating the expression of *Irf7*, *Irf3*, *Stat1*, *Cxcl10*, *Mbl2*, *Lyz2*, and *Ccr5*. The mechanisms by which the *Pparg* product suppresses genes involved in the TLR pathway and defense response (i.e., innate immunity) warrant further investigation.

Regarding fatty liver, *Pparg* overexpression has been observed in several animal models of obesity and diabetes [40,41]. The liver regulates lipid homeostasis by controlling lipid uptake from the circulatory system, de novo synthesis, and the delivery of synthesized lipids to peripheral tissues as very low-density lipoprotein [42]. We previously proposed that LPS contributes to hepatic steatosis by binding to TG-rich lipoproteins and allowing them to be removed from the systemic circulation more quickly by liver hepatocytes [43]. These new findings support the hypothesis that bacterial LPS also contributes to fatty liver via the stimulation of *Pparg* overexpression. Indeed, *Pparg* has been shown to play a direct role in TG and lipid droplet formation in vivo [44,45].

Annotation cluster analysis revealed that up-regulated liver genes like *Kras*, *Rras2*, *Raf1*, *Frs3*, *Gsk3b*, *Hk2*, and *Pik3r2* are involved in the 'B-cell receptor signaling pathway', the 'T-cell receptor signaling pathway', and the 'chemokine signaling pathway'. The liver is home to a variety of immune cells, including Kupfer cells, natural killer (NK) cells, and T and B lymphocytes [46]. Based on our findings, it is evident that despite the administration of LPS at a significantly low concentration for a duration of 6 weeks starting at the age of 35 days, long-lasting alterations were observed in the expression of genes associated with the 'B-cell receptor signaling pathway', the 'T-cell receptor signaling pathway', and the 'chemokine signaling pathway'.

LPS treatment induced cancer-related genes in the liver, including *Kras*, *Rras2*, and *Raf1*. KRAS is required for normal cell signaling, growth, proliferation, and apoptosis, and mutations in this gene have been linked to a variety of human cancers [47,48]. Somatic activation of the *Kras* oncogene causes lung cancer to develop early in mice [49], and its transcription levels have been linked to a variety of cancers, including cystadenocarcinoma and prostate cancer [50,51]. *Rras2* has been linked to ovarian cancer and chronic lymphocytic leukemia [52,53]. Furthermore, *Raf1* has been linked to tumors of the parotid gland, stomach cancer, and renal cell carcinoma [54–56]. According to the annotation cluster analysis, upregulation of three genes, namely *Kras*, *Gsk3b*, and *Raf1*, was observed in LPS-treated mice. These genes are associated with pathways related to 'endometrial cancer,' 'colorectal cancer,' and 'prostate cancer'.

Jiang et al. [57] reported that endotoxin levels in human blood increased significantly with the progression of liver cancer, with the highest level found in the advanced liver cancer group. Another study, Liu et al. [58], concluded that LPS in the chronic liver inflammation microenvironment may play a role in hepatocarcinogenesis by regulating the plastic potential of hepatic progenitor cells. To the best of our knowledge, this is the first study to show that chronic LPS administration early in life upregulates genes associated with cancer pathways in mouse liver tissue nearly two years later.

The up-regulation of genes *Gsk3b* (glycogen synthase kinase-3), *Hk2* (hexokinase 2), and *Pik3r2* (phosphatidylinositol 3-kinase regulatory subunit beta) in the liver of mice treated with LPS is important for the regulation of the activities of both innate and adaptive immune cells during inflammation and disease. GSK3, for example, is involved in the production of pro-inflammatory cytokines in response to TLR stimulation [59]. When pathogens are detected by the innate immune system, inflammation is initiated. Bacteria are phagocytosed by both resident macrophages and infiltrating neutrophils using a variety of cell surface receptors. To kill engulfed bacteria, neutrophils activate an intracellular NADPH oxidase, which produces reactive oxygen species (ROS). Each of these processes necessitates the activation of class I Pi3k [60]. GSK3 deficiency caused by lithium or other *Gsk3* inhibitors, or molecular manipulation, decreases proinflammatory cytokine production by TLR-stimulated monocytes by 67–90% [59]. Moreover, *Hk2* supports neoplastic growth in glioblastoma multiforme [61], provides chemoresistance to epithelial cells of ovarian cancer [62], and initiates and maintains lung and breast cancer tumors in lung and breast mouse models, and its inhibition confers therapeutic effects [63].

The spleen is also considered to be an important organ in the removal of LPS from systemic circulation. Indeed, LPS administered intravenously to rats was detected in decreasing concentrations in spleen macrophages between 24 h and a week after admin-

istration [64]. Groeneveld and van Rooijen [65] previously reported the distribution of intravenously administered radiolabeled LPS in the spleen of mice. The majority of the LPS was accumulated in macrophages in the splenic marginal zone (MZ). Furthermore, LPS reduced MZ macrophages and eliminated lymphocytes from the marginal zone. Extracellular dendritic localization of LPS in the central parts of spleen follicles, on the other hand, has been reported. These findings are significant because they show that intravenous LPS is captured by splenic immune cells, primarily resident macrophages, and dendritic cells.

According to gene expression profiling in our study, long-term subcutaneous administration of LPS in female mice up-regulated 12 genes and down-regulated 11 genes in the spleen tissue. 'Inflammatory response' was the most enriched GO (gene ontology) term, and the most up-regulated pathways in the spleen were 'viral protein interaction with cytokines and cytokine receptors', 'chemokine receptors bind chemokines' and 'cytokine–cytokine receptor interaction' with the genes *Ccl11*, *Ccl17*, *Ccl25*, *Cxcl5*, *Cxcl11*, *Il6* and *Il-1a*. The first five genes encode critical chemokines, while the remaining two genes encode two key proinflammatory cytokines, interleukin (IL)-6 and IL-1a. Chemokines are a large family of small cytokines that can interact with chemokine receptors, which control immune cell residence and migration and are involved in immunoregulatory and inflammatory processes.

The *Ccl11* gene is up-regulated in response to an increase in the concentration of C-C motif chemokine 11, also known as eotaxin. CCL11 has the highest affinity for the C-C chemokine receptor CCR3, as well as CCR2 and CCR5 [66,67]. It has been reported that CCL11 induces the migration of several types of leukocytes, including eosinophils, basophils, macrophages, and dendritic cells, via interaction with CCR3 [68–71]. Earlier studies have shown that *Ccl11* is activated by pro-inflammatory cytokines such as tumor necrosis factor (TNF) [72–74]. CCL11 is also a strong inducer of eosinophil chemotaxis, which results in eosinophil migration in vitro and accumulation in vivo. A recent study by Xu et al. [75] found that a significant number of eosinophils were recruited to the liver during experimental liver failure in mice, compared to very few eosinophils in normal livers. Plötz et al. [76] discovered that LPS stimulates TNF secretion from eosinophils as well as LPS uptake via the CD14 pathway. There is an increase in the number of eosinophils in the blood circulation in patients who have had a splenectomy [77], indicating the importance of the spleen in controlling the number of eosinophils. Eosinophils are highly active inflammatory cells that produce and secrete a wide range of mediators leading to cytotoxic activity and tissue damage [78,79].

Overexpression of *Ccl17* is intriguing because it interacts with a high-affinity receptor found on T cells and, to a lesser extent, monocytes. This is a chemokine that plays a role in both innate and adaptive immune regulation. CCL17 attracts both natural killer cells and dendritic cells. This chemokine is also important because it attracts Th2 cells and suppresses type 1 innate immune responses while stimulating type 2 immune responses [80]. While type 1 immune responses are characterized by the activation of M1 macrophages associated with phagocytic activity, type 2 immune responses are associated with the activation of M2 macrophages associated with humoral immunity [80]. It is likely that early-life parenteral LPS treatment of mice resulted in long-term changes in the expression of chemokines that promote humoral immune responses to blood-borne LPS.

C-C chemokine ligand 25 (*Ccl25*) was another overexpressed gene in LPS-treated mice. C-C chemokine receptor 9 (CCR9) is the receptor for CCL25. Because this chemokine is secreted by only a few cell populations, CCL25 synthesis is tightly controlled. *Ccl25* mRNA is primarily expressed in the thymus and small intestine of mice, with low levels found in the liver, brain, testis, and effector T cells [81]. Our study is one of the few to show that subcutaneously administering LPS at a young age causes long-term changes in gene expression profiling in spleen tissue, with *Ccl25* being up-regulated in the treated mice. Meanwhile, [81] reported that LPS stimulates *Ccl25* expression in the spleen of mice in vivo. In the thymus, the CCR9 receptor is involved in T-cell development and trafficking [82]. *Ccl25* is also produced by dendritic cells and epithelial cells in the thymus

and possibly in the spleen [83]. *Ccl25*, which is expressed in the small intestinal epithelium, aids in the recruitment of T and B cells that express the CCR9 receptor [84]. According to Eksteen et al. [85], CCL25 was found in high concentrations in hepatic blood vessels in inflamed livers. The overexpression of *Ccl25* in spleen tissue is thought to play a similar role in the recruitment of T and B cells into the spleen.

One of the up-regulated genes in the spleen of mice treated with subcutaneous LPS was *Cxcl5*. The protein encoded by *Cxcl5* (epithelial cell-derived neutrophil attractant) is a chemokine that has been demonstrated to attract neutrophils at the site of infection. In a study by Jeyaseelan et al. [86], mice were treated with aerosolized LPS to induce acute lung injury. The authors reported an overexpression of *Cxcl5*. Acute lung injury is characterized by an abnormally high neutrophil influx into the lungs, which has been linked to increased blood endotoxin concentrations as well as endothelial and epithelial damage in the lungs. Previous studies have indicated that FVB/N mice exhibit higher susceptibility to lung tumors while being comparatively less susceptible to liver tumors and lymphomas when compared to other mouse strains [87]. However, it is important to note that in our study, we employed the same genotype, ensuring that any observed results are primarily attributed to the effects of LPS treatment rather than the influence of the genotype. Although there are no data on the effects of LPS on *Cxcl5* in the spleen, *Cxcl5* overexpression in the spleen of mice in our experiment could be a response to subcutaneous LPS to attract neutrophils to the spleen. In this study, we did not collect data on the incidence of cancer, diabetes, and/or steatosis. Consequently, future studies are crucial to investigate and determine the potential role of LPS in the development and occurrence of these diseases.

Overall, the mechanism by which early-life subcutaneous administration of LPS for 6 weeks in female FVB/N mice caused long-term changes in gene expression of various chemokines and chemokine receptors in the liver and spleen is unknown; we believe that LPS caused epigenetic changes in the liver and spleen cells of the treated mice. This hypothesis is supported by recent studies using bovine cells treated with LPS and reporting that the latter induces DNA methylation. A study of bovine endometrial cells treated with LPS, for example, discovered that LPS induced DNA methylation patterns in bovine endometrial epithelial cells as well as activated proinflammatory mechanisms that disrupted immune balance and endometrial adhesion processes [88]. Another study discovered that low doses of bacterial LPS caused DNA hypomethylation in bovine mammary epithelial cells, while high doses caused hypermethylation [89].

## 5. Conclusions

In summary, our findings suggest that early-life (35-day old) exposure to chronic and continuous (for 6 weeks) endotoxemia may initiate molecular mechanisms that lead to long-term differential gene expression changes related to inflammation and adaptive immunity and may be involved in the pathobiology of a variety of chronic inflammatory diseases in the liver and spleen. Chronic endotoxemia may also contribute to hepatic steatosis and liver cancer in LPS-treated mice, according to our findings. Changes in gene expression related to energy metabolism, the suppression of TLR and immune responses, and the upregulation of genes related to B-cell and T-cell receptors, as well as chemokine signaling pathways, may all result from LPS treatment. The spleen plays a role in chronic endotoxemia response by removing LPS from circulation, establishing innate and adaptive immune responses, recruiting eosinophils and T cells, and promoting humoral immune responses. More research using a greater number of animals is needed to understand the long-term effects of early endotoxin exposure on gene expression in the liver, spleen, and possibly other organs.

**Supplementary Materials:** The following supporting information can be downloaded at: <https://www.mdpi.com/article/10.3390/vetsci10070445/s1>, Figure S1: The weight of the mice treated with lipopolysaccharide (LPS) and control (CON) during the experimental period.

**Author Contributions:** Conceptualization, B.N.A.; methodology, B.N.A.; investigation, B.N.A., E.D., D.H. and S.A.G.; resources, B.N.A.; data curation, E.D.; writing—original draft preparation, E.D.; writing—review and editing, B.N.A., E.D., D.H. and S.A.G.; supervision, B.N.A.; project administration, B.N.A.; funding acquisition, B.N.A. All authors have read and agreed to the published version of the manuscript.

**Funding:** Alberta Livestock and Meat Agency Ltd. (ALMA) and Alberta Prion Research Institute (APRI) funded the research (4 March 2011), grant number 2010R068R.

**Institutional Review Board Statement:** All the protocols used during the study were in accordance with the Canadian Council on Animal Care and were approved by the Animal Care and Use Committee (Animal Use Protocol #660), Health Sciences, University of Alberta.

**Informed Consent Statement:** Not applicable.

**Data Availability Statement:** All data analyzed during this study are included in this published article.

**Acknowledgments:** We acknowledge the technical support given by the staff of The Centre for Prions and Protein Folding Disease (CPPFD) at the University of Alberta in caring for the animals.

**Conflicts of Interest:** The authors declare no conflict of interest.

## References

- Nikaido, H. Outer membrane. In *Escherichia Coli and Salmonella: Cellular and Molecular Biology*, 2nd ed.; Neidhardt, F.C., Curtiss, R., III, Ingraham, J.L., Lin, E.C.C., Low, K.B., Jr., Magasanik, B., Reznikoff, W.S., Riley, M., Schaechter, M., Umberger, H.E., Eds.; American Society for Microbiology: Washington, DC, USA, 1992; pp. 29–47.
- Rietschel, E.T.; Kirikae, T.; Schade, F.U.; Mamat, U.; Schmidt, G.; Loppnow, H.; Ulmer, A.J.; Zahringer, U.; Seydel, U.; Di Padova, F. Bacterial endotoxin: Molecular relationships of structure to activity and function. *FASEB J.* **1994**, *8*, 217–225. [[CrossRef](#)] [[PubMed](#)]
- Rietschel, E.T.; Brade, H. Bacterial endotoxins. *Sci. Am.* **1992**, *267*, 26–33. [[CrossRef](#)] [[PubMed](#)]
- Galanos, C.; Freudenberg, M.A.; Katschinski, T.; Salomao, R.; Mossmann, H.; Kumazawa, Y. Tumor necrosis factor and host response to endotoxin. In *Bacterial Endotoxic Lipopolysaccharides, Immunopharmacology and Pathophysiology*; Ryan, J.L., Morrison, D.C., Eds.; CRC Press: Boca Raton, FL, USA, 1992; Volume 2, pp. 75–102.
- Galanos, C.; Freudenberg, M.A. Mechanisms of endotoxin shock and endotoxin hypersensitivity. *Immunobiology* **1993**, *187*, 346–356. [[CrossRef](#)] [[PubMed](#)]
- Gordon, S. Pattern recognition receptors. Doubling up for the innate immune response. *Cell* **2002**, *111*, 927–930. [[CrossRef](#)] [[PubMed](#)]
- Janeway, C.A.; Madzhitov, R. Innate immune recognition. *Annu. Rev. Immunol.* **2002**, *20*, 197–216. [[CrossRef](#)] [[PubMed](#)]
- Yang, R.B.; Mark, M.R.; Gray, A.; Huang, A.; Hong, X.M.; Zhang, M.; Goddard, A.; Wood, W.I.; Gurney, A.L.; Godowski, P.J. Toll like receptor-2 mediates lipopolysaccharide—Induced cellular signaling. *Nature* **1998**, *395*, 284–288. [[CrossRef](#)]
- Chow, J.C.; Young, D.W.; Golenbock, D.T.; Christ, W.J.; Gusovsky, F. Toll-like receptor-4 mediates lipopolysaccharide-induced signal transduction. *J. Biol. Chem.* **1999**, *274*, 10689–10692. [[CrossRef](#)]
- Vogel, S.N.; Hogan, M.M. The role of cytokines in endotoxin- mediated host responses. In *Immunopharmacology. The role of Cells and Cytokines in Immunity and Inflammation*; Oppenheim, J.J., Shevack, E.M., Eds.; Oxford University Press: New York, NY, USA, 1990; pp. 238–258.
- Duncan, B.B.; Schmidt, M.I.; Pankow, J.S.; Ballantyne, C.M.; Couper, D.; Vigo, A.; Hoogeveen, R.; Folsom, A.R.; Heiss, G. Low grade systemic inflammation and the development of type 2 diabetes. The atherosclerosis risk in communities study. *Diabetes* **2003**, *52*, 1799–1805. [[CrossRef](#)]
- Cani, P.D.; Amar, J.; Iglesias, M.G.; Poggi, M.; Knauf, C.; Bastelica, D.; Myrinck, A.M.; Fava, F.; Tuohy, K.M.; Chabo, C.; et al. Metabolic endotoxemia initiates obesity and insulin resistance. *Diabetes* **2007**, *7*, 1761–1772. [[CrossRef](#)]
- Nakarai, H.; Yamashita, A.; Nagayasu, S.; Iwashita, M.; Kumamoto, S.; Ohyama, H.; Hata, M.; Soga, Y.; Kushiya, A.; Asano, T.; et al. Adipocyte- macrophage interaction may mediate LPS- induced low-grade inflammation: Potential link with metabolic complications. *Innate Immun.* **2012**, *18*, 164–170. [[CrossRef](#)]
- Ridker, P.M.; Cushman, M.; Stampfer, M.J.; Trancey, R.P.; Hennekens, C.H. Inflammation, aspirin and the risk of cardiovascular disease in apparently healthy men. *N. Engl. J. Med.* **1997**, *336*, 973–979. [[CrossRef](#)] [[PubMed](#)]
- Xu, X.H.; Shah, P.K.; Faure, E.; Equils, O.; Thomas, L.; Fishbein, M.C.; Luthringer, D.; Xu, X.P.; Rajavashisth, T.B.; Yano, J.; et al. Toll like receptor 4 is expressed by macrophages in murine and human lipid- rich atherosclerotic plaques and up-regulated by oxidized LDL. *Circulation* **2001**, *104*, 3103–3108. [[CrossRef](#)] [[PubMed](#)]
- Edfeld, K.; Swedenborg, J.; Hansson, G.K.; Yan, Q.K. Expression of Toll-like receptors in human atherosclerotic lesions: A possible pathway for plaque activation. *Circulation* **2002**, *105*, 1158–1161. [[CrossRef](#)]
- Hansson, G.K.; Libby, P.; Schonbeck, U.; Yan, Z.Q. Innate and adaptive immunity in the pathogenesis of atherosclerosis. *Circulation* **2002**, *91*, 281–291. [[CrossRef](#)] [[PubMed](#)]

18. Ikebe, M.; Kitaura, Y.; Nakamura, M.; Tanaka, H.; Yamaski, A.; Nagai, S.; Wada, J.; Yanai, K.; Koga, K.; Sato, N.; et al. Liposaccharide (LPS) increases the invasive ability of pancreatic cancer cell through the TLR4/ MyD88 signaling pathway. *J. Surgical Onc.* **2009**, *100*, 725–731. [[CrossRef](#)] [[PubMed](#)]
19. Hsu, R.Y.; Chan, C.H.; Spicer, J.D.; Rousseau, M.C.; Giannias, B.; Rousseau, S.; Ferri, L.E. LPS-induced TLR4 signaling in human colorectal cancer cells increases beta1 integrin-mediated cell adhesion and liver metastasis. *Cancer Res.* **2011**, *71*, 1989–1998. [[CrossRef](#)]
20. Ma, K.L.; Ruan, X.Z.; Powis, S.H.; Chen, Y.; Moorhead, J.F.; Varghese, Z. Inflammatory stress exacerbates lipid accumulation in hepatic cells and fatty livers of apolipoprotein E knockout mice. *Hepatology* **2008**, *48*, 770–781. [[CrossRef](#)] [[PubMed](#)]
21. Schaffert, C.S.; Duryee, M.J.; Thiele, G.M. Alcohol metabolites and lipopolysaccharide: Role in the development and/or progression of alcoholic liver disease. *World J. Gastroenterol.* **2009**, *15*, 1209–1218. [[CrossRef](#)] [[PubMed](#)]
22. Straub, R.H. Complexity of the bi-directional neuroimmune junction in the spleen. *Trends Pharmacol. Sci.* **2004**, *25*, 640–646. [[CrossRef](#)]
23. Lewis, S.M.; Williams, A.; Eisenbarth, S.C. Structure and function of the immune system in the spleen. *Sci. Immunol.* **2019**, *4*, eaau6085. [[CrossRef](#)] [[PubMed](#)]
24. Ehlting, C.; Wolf, S.D.; Bode, J.G. Acute-phase protein synthesis: A key feature of innate immune functions of the liver. *Biol. Chem.* **2021**, *402*, 1129–1145. [[CrossRef](#)] [[PubMed](#)]
25. Olfert, E.D.; Cross, B.M.; McWilliam, A.A. The Guide to the care and use of experimental Animals. *Can. Counc. Anim. Care* **1993**, *1*, 19–22.
26. Hailemariam, D.; Goldansaz, S.A.; Daude, N.; Wishart, D.S.; Ametaj, B.N. Mice treated subcutaneously with mouse LPS-converted PrPres or LPS alone showed brain gene expression profiles characteristic of prion disease. *Vet. Sci.* **2021**, *8*, 200. [[CrossRef](#)] [[PubMed](#)]
27. Xia, J.; Psychogios, N.; Young, N.; Wishart, D.S. Metaboanalyst: A web server for metabolomic data analysis and interpretation. *Nucleic Acids Res.* **2009**, *37*, 652–660. [[CrossRef](#)] [[PubMed](#)]
28. Huang, D.W.; Sherman, B.T.; Lempicki, R.A. Systematic and integrative analysis of large gene lists using DAVID bioinformatics resources. *Nature Prot.* **2008**, *4*, 44–57. [[CrossRef](#)]
29. Sherman, B.T.; Hao, M.; Qiu, J.; Jiao, X.; Baseler, M.W.; Lane, H.C.; Imamichi T.; Chang, W. DAVID: A web server for functional enrichment analysis and functional annotation of gene lists (2021 update). *Nucleic Acids Res.* **2022**, *50*, W216–W221. [[CrossRef](#)] [[PubMed](#)]
30. Bindea, G.; Mlecnik, B.; Hackl, H.; Charoentong, P.; Tosolini, M.; Kirilovsky, A.; Fridman, W.H.; Pagès, F.; Trajanoski, Z.; Galon, J. ClueGO: A Cytoscape plug-in to decipher functionally grouped gene ontology and pathway annotation networks. *Bioinformatics* **2009**, *15*, 1091–1093. [[CrossRef](#)]
31. Shannon, P.; Markiel, A.; Ozier, O.; Baliga, N.S.; Wang, J.T.; Ramage, D.; Amin, N.; Schwikowski, B.; Ideker, T. Cytoscape: A software environment for integrated models of biomolecular interaction networks. *Genome Res.* **2003**, *13*, 2498–2504. [[CrossRef](#)] [[PubMed](#)]
32. Warner, A.E.; Brain, J.D. Intravascular pulmonary macro-phages: A novel cell removes particles from blood. *Am. J. Physiol. Reg. Integr. Comp. Physiol.* **1986**, *1250*, R728–R732. [[CrossRef](#)]
33. Mathison, J.C.; Ulevitch, R.J. The clearance, tissue distribution, and cellular localization of intravenously injected lipopolysaccharide in rabbits. *J. Immunol.* **1979**, *123*, 2133–2143. [[CrossRef](#)]
34. Evans, R.M.; Barish, G.D.; Wang, Y.X. PPARs and the complex journey to obesity. *Nature Rev.* **2004**, *10*, 355–361.
35. Su, C.G.; Wen, X.; Bailey, S.T.; Jiang, W.; Rangwala, S.M.; Keilbaugh, S.A.; Flanigan, A.; Murthy, S.; Lazar, M.A.; Wu, G.D. A novel therapy for colitis utilizing PPAR- $\gamma$  ligands to inhibited the epithelial inflammatory response. *J. Clin. Investig.* **1999**, *104*, 383–389. [[CrossRef](#)]
36. Zingarelli, B.; Sheehan, M.; Hake, P.W.; O'Connor, M.; Denenberg, A.; Cook, J.A. Peroxisome proliferator activator receptor- $\gamma$  ligands 15-deoxy- 12, 14- prostaglandine J2 and ciglitazone, reduce systemic inflammation in polymicrobial sepsis by modulation of signal transduction pathways. *J. Immunol.* **2003**, *171*, 6827–6837. [[CrossRef](#)]
37. Abdelrahman, M.; Collin, M.; Thiemermann, C. The peroxisome proliferator- activated receptor-  $\gamma$  ligand 15- deoxy-12,14 prostaglandine J2, reduces the organ injury in hemorrhagic shock. *Shock* **2004**, *22*, 555–561. [[CrossRef](#)] [[PubMed](#)]
38. Siddiqui, A.M.; Cui, X.; Wu, R.; Dong, W.; Zhou, M.; Hu, M.; Simms, H.H.; Wang, P. The anti-inflammatory effect of curcumin in an experimental model of sepsis is mediated by up- regulation of peroxisome proliferator activated receptor-  $\gamma$ . *Crit. Car. Med.* **2006**, *34*, 1874–1882. [[CrossRef](#)] [[PubMed](#)]
39. Zhou, M.; Wu, R.; Dong, W.; Jacob, A.; Wang, P. Endotoxin down- regulates peroxisome proliferator- activated gamma via the increase in TNF- alpha release. *Am. J. Physiol.* **2008**, *294*, 84–92.
40. Memon, R.A.; Tecott, L.H.; Nonogaki, K.; Beigneux, A.; Moser, A.H.; Grunfeld, C.; Feingold, K.R. Up-regulation of peroxisome proliferator-activated receptors (PPAR-alpha) and PPAR-gamma messenger ribonucleic acid expression in the liver in murine obesity: Troglitazone induces expression of PPAR-gamma-responsive adipose tissue-specific genes in the liver of obese diabetic mice. *Endocrinology* **2000**, *141*, 4021–4031. [[PubMed](#)]
41. Bedoucha, M.; Atzpodien, E.; Boelsterli, U.A. Diabetic KKAy mice exhibit increase hepatic PPAR $\gamma$ 1 gene expression and develop hepatic steatosis upon chronic treatment with antidiabetic thiazolidinediones. *J. Hepat.* **2001**, *35*, 17–23. [[CrossRef](#)] [[PubMed](#)]

42. Browning, J.D.; Horton, J.D. Molecular mediators of hepatic steatosis and liver injury. *J. Clin. Invest.* **2004**, *114*, 147–152. [[CrossRef](#)] [[PubMed](#)]
43. Eckel, E.F.; Ametaj, B.N. Invited review: Role of bacterial endotoxins in the etiopathogenesis of periparturient diseases of transition dairy cows. *J. Dairy. Sci.* **2016**, *99*, 5967–5990. [[CrossRef](#)]
44. Neuschwander-Tetri, B.A. Hepatic lipotoxicity and the pathogenesis of nonalcoholic steatohepatitis: The central role of non-triglyceride fatty acid metabolites. *Hepatology* **2010**, *52*, 774–788. [[CrossRef](#)] [[PubMed](#)]
45. Wang, Y.; Nakajima, T.; Gonzalez, F.J.; Tanaka, N. PPARs as metabolic regulators in the liver: Lessons from liver-specific PPAR-null mice. *Int. J. Mol. Sci.* **2020**, *21*, 2061. [[CrossRef](#)] [[PubMed](#)]
46. Jenne, C.N.; Kubes, P. Immune surveillance by the liver. *Nat. Immunol.* **2013**, *14*, 996–1006. [[CrossRef](#)] [[PubMed](#)]
47. Weinberg, R.A. Fewer and fewer oncogenes. *Cell* **1982**, *30*, 3–4. [[CrossRef](#)] [[PubMed](#)]
48. Kranenburg, O. The KRAS oncogene: Past, present, and future. *Biochim. Biophys. Acta* **2005**, *1756*, 81–82. [[CrossRef](#)] [[PubMed](#)]
49. Johnson, L.; Mercer, K.; Greenbaum, D.; Roderick, T.; Bronson, R.T.; Crowley, D.; Tuveson, A.D.; Jacks, T. Somatic activation of the K-ras oncogene causes early onset lung cancer in mice. *Nature* **2001**, *410*, 1111–1116. [[CrossRef](#)]
50. Feig, L.; Bast, R.C.; Knapp, R.C.; Cooper, G.M. Somatic activation of ras K gene in human ovarian carcinoma. *Science* **1984**, *223*, 698–701. [[CrossRef](#)]
51. Poliseno, L.; Salmena, L.; Zhang, J.; Carve, B.; Haveman, W.J.; Pandolfi, P.P. A coding-independent function of gene and pseudogene mRNA regulates tumor biology. *Nature* **2010**, *465*, 1033–1038. [[CrossRef](#)]
52. Chan, A.M.; Miki, T.; Meyers, K.A.; Aaronson, S.A. A human oncogene of the RAS superfamily unmasked by expression cDNA cloning. *Proc. Natl. Acad. Sci. USA* **1994**, *91*, 7558–7562. [[CrossRef](#)]
53. Hortal, A.M.; Oeste, C.L.; Cifuentes, C.; Alcoceba, M.; Fernández-Pisonero, I.; Clavain, L.; Tercero, R.; Mendoza, P.; Domínguez, V.; García-Flores, M.; et al. Overexpression of wild type RRAS2, without oncogenic mutations, drives chronic lymphocytic leukemia. *Mol Cancer* **2022**, *21*, 35. [[CrossRef](#)]
54. Bonner, T.; O'Brien, S.J.; Nash, W.G.; Rapp, U.R.; Morton, C.C.; Leder, P. The human homologs of the raf (mil) oncogene are located on human chromosomes 3 and 4. *Science* **1984**, *223*, 71–74. [[CrossRef](#)] [[PubMed](#)]
55. Shimizu, K.; Nakatsu, Y.; Sekiguchi, M.; Hokamura, K.; Tanaka, K.; Terada, M.; Sugimura, T. Molecular cloning of an activated human oncogene, homologous to v-raf, from primary stomach cancer. *Proc. Natl. Acad. Sci. USA* **1985**, *82*, 5641–5645. [[CrossRef](#)] [[PubMed](#)]
56. Teyssier, J.R.; Henry, I.; Dozier, C.; Ferre, D.; Adnet, J.J.; Pluot, M. Recurrent deletion of the short arm of chromosome 3 in human cell carcinoma: Shift of the c-raf1 locus. *J. Nat. Cancer Inst.* **1986**, *77*, 1187–1191. [[PubMed](#)]
57. Jiang, N.; Song, X.; Peng, Y.M.; Wang, W.N.; Song, Z. Association of disease condition with changes in intestinal flora, and plasma endotoxin and vascular endothelial growth factor levels in patients with liver cancer. *Eur. Rev. Med. Pharmacol. Sci.* **2020**, *24*, 3605–3613.
58. Liu, W.T.; Jing, Y.Y.; Gao, L.; Li, R.; Yang, X.; Pan, X.R.; Yang, Y.; Meng, Y.; Hou, X.J.; Zhao, Q.D.; et al. Lipopolysaccharide induces the differentiation of hepatic progenitor cells into myofibroblasts constitutes the hepatocarcinogenesis-associated microenvironment. *Cell Death Differ.* **2020**, *27*, 85–101. [[CrossRef](#)]
59. Martin, M.; Rehani, K.; Jope, R.S.; Michalek, S.M. Toll-like receptor-mediated cytokine production is differentially regulated by glycogen synthase kinase 3. *Nat Immunol.* **2005**, *6*, 777–784. [[CrossRef](#)]
60. Hawkins, P.T.; Stephens, L.R. PI3K signalling in inflammation. *Biochem. Biophys. Acta.* **2015**, *51*, 882–897. [[CrossRef](#)] [[PubMed](#)]
61. Wolf, A.; Agnihotri, S.; Micallef, J.; Mukherjee, J.; Sabha, N.; Cairns, R.; Hawkins, C.; Guha, A. Hexokinase 2 is a key mediator of aerobic glycolysis and promotes tumor growth in human glioblastoma multiforme. *J. Exp. Med.* **2011**, *208*, 313–326. [[CrossRef](#)]
62. Suh, D.H.; Kim, M.A.; Kim, H.; Kim, M.K.; Kim, H.S.; Chung, H.H.; Kim, Y.B.; Song, Y.S. Association of overexpression of hexokinase II with chemoresistance in epithelial ovarian cancer. *Clin. Exp. Med.* **2014**, *14*, 345–353. [[CrossRef](#)]
63. Patra, K.C.; Wang, Q.; Bhaskar, P.T.; Miller, L.; Wang, Z.; Wheaton, W.; Chandel, N.; Laakso, M.; Muller, W.J.; Allen, E.L.; et al. Hexokinase 2 is required for tumor initiation and maintenance and its systemic deletion is therapeutic in mouse models of cancer. *Cancer Cell* **2013**, *24*, 213–228, Erratum in *Cancer Cell* **2013**, *24*, 399. [[CrossRef](#)]
64. Ge, Y.; Ezzell, R.M.; Clark, B.D.; Loisel, P.M.; Amato, S.F.; Warren, H.S. Relationship of tissue and cellular interleukin-1 and lipopolysaccharide after endotoxemia and bacteremia. *J. Infect. Dis.* **1997**, *176*, 1313–1321. [[CrossRef](#)] [[PubMed](#)]
65. Groeneveld, P.H.; van Rooijen, N. Localization of intravenously injected lipopolysaccharide (LPS) in the spleen of the mouse. An immunoperoxidase and histochemical study. *Virchows Arch. B Cell Pathol. Incl. Mol. Pathol.* **1985**, *48*, 237–245. [[CrossRef](#)] [[PubMed](#)]
66. Kitaura, M.; Nakajima, T.; Imai, T.; Harada, S.; Combadiere, C.; Tiffany, H.L.; Murphy, P.M.; Yoshie, O. Molecular cloning of human eotaxin, an eosinophil-selective CC chemokine, and identification of a specific eosinophil eotaxin receptor, CC chemokine receptor 3. *J. Biol. Chem.* **1996**, *271*, 7725–7730. [[CrossRef](#)]
67. Ye, J.; Kohli, L.L.; Stone, M.J. Characterization of binding between the chemokine eotaxin and peptides derived from the chemokine receptor CCR3. *J. Biol. Chem.* **2000**, *275*, 27250–27257. [[CrossRef](#)] [[PubMed](#)]
68. Elsner, J.; Hochstetter, R.; Kimmig, D.; Kapp, A. Human eotaxin represents a potent activator of the respiratory burst of human eosinophils. *Eur. J. Immunol.* **1996**, *26*, 1919–1925. [[CrossRef](#)] [[PubMed](#)]



69. Ugucioni, M.; Mackay, C.R.; Ochensberger, B.; Loetscher, P.; Rhis, S.; LaRosa, G.J.; Rao, P.; Ponath, P.D.; Baggiolini, M.; Dahinden, C.A. High expression of the chemokine receptor CCR3 in human blood basophils. Role in activation by eotaxin, MCP-4, and other chemokines. *J. Clin. Invest.* **1997**, *100*, 1137–1143. [[CrossRef](#)] [[PubMed](#)]
70. Peled, A.; Gonzalo, J.A.; Lloyd, C.; Gutierrez-Ramos, J.C. The chemotactic cytokine eotaxin acts as a granulocyte-macrophage colony-stimulating factor during lung inflammation. *Blood* **1998**, *91*, 1909–1916. [[CrossRef](#)] [[PubMed](#)]
71. Menzies-Gow, A.; Ying, S.; Sabroe, I.; Stubbs, V.L.; Soler, D.; Williams, T.J.; Kay, A.B. Eotaxin (CCL11) and eotaxin-2 (CCL24) induce recruitment of eosinophils, basophils, neutrophils, and macrophages as well as features of early- and late-phase allergic reactions following cutaneous injection in human atopic and nonatopic volunteers. *J. Immunol.* **2002**, *169*, 2712–2718. [[CrossRef](#)]
72. Lilly, C.M.; Nakamura, H.; Kesselman, H.; Nagler-Anderson, C.; Asano, K.; Garcia-Zepeda, E.A.; Rothenberg, M.E.; Drazen, J.M.; Luster, A.D. Expression of eotaxin by human lung epithelial cells: Induction by cytokines and inhibition by glucocorticoids. *J. Clin. Invest.* **1997**, *99*, 1767–1773. [[CrossRef](#)]
73. Bartels, J.; Schlüter, C.; Richter, E.; Noso, N.; Kulke, R.; Christophers, E.; Schröder, J.M. Human dermal fibroblasts express eotaxin: Molecular cloning, mRNA expression, and identification of eotaxin sequence variants. *Biochem. Biophys. Res. Commun.* **1996**, *225*, 1045–1051. [[CrossRef](#)]
74. Miyamasu, M.; Nakajima, T.; Misaki, Y.; Izumi, S.; Tsuno, N.; Kasahara, T.; Yamamoto, K.; Morita, Y.; Hirai, K. Dermal fibroblasts represent a potent major source of human eotaxin: In vitro production and cytokine-mediated regulation. *Cytokine* **1999**, *11*, 751–758. [[CrossRef](#)]
75. Xu, L.; Yang, Y.; Wen, Y.; Jeong, J.M.; Emontz pohl, C.; Atkins, C.L.; Sun, Z.; Poulsen, K.L.; Hall, D.R.; Steve Bynon, J.; et al. Hepatic recruitment of eosinophils and their protective function during acute liver injury. *J. Hepatol.* **2022**, *77*, 344–352. [[CrossRef](#)]
76. Plötz, S.G.; Lentschat, A.; Behrendt, H.; Plötz, W.; Hamann, L.; Ring, J.; Rietschel, E.T.; Flad, H.D.; Ulmer, A.J. The interaction of human peripheral blood eosinophils with bacterial lipopolysaccharide is CD14 dependent. *Blood* **2001**, *97*, 235–241. [[CrossRef](#)]
77. Perl, L.; Pasvolosky, O.; Lifshitz, L.; Mekori, Y.A.; Hershko, A.Y. Increased eosinophilic responses in splenectomized patients. *Ann. Allergy Asthma Immunol.* **2012**, *108*, 34–38. [[CrossRef](#)]
78. Blanchard, C.; Rothenberg, M.E. Biology of the eosinophil. *Adv. Immunol.* **2007**, *27*, 357–375.
79. Spencer, L.A.; Szela, C.T.; Perez, S.A.; Kirchhoffer, C.L.; Neves, J.S.; Radke, A.L.; Weller, P.F. Human eosinophils constitutively express multiple Th1, Th2, and immunoregulatory cytokines that are secreted rapidly and differentially. *J. Leukoc. Biol.* **2009**, *85*, 117–123. [[CrossRef](#)]
80. Ness, T.L.; Hogaboam, C.M.; Kunkel, S.L. Chemokines: TARC (CCL17). In *Encyclopedia of Respiratory Medicine*, 1st ed.; Laurent, G.J., Shapiro, S.D., Eds.; Academic Press: Cambridge, MA, USA, 2006; pp. 380–384.
81. Buckland, K.F.; Hogaboam, C.M. TECK (Ccl25). In *Encyclopedia of Respiratory Medicine*, 2nd ed.; Academic Press: Cambridge, MA, USA, 2006; pp. 385–389.
82. Vicari, A.P.; Figueroa, D.J.; Hedrick, J.A.; Foster, J.S.; Singh, K.P.; Menon, S.; Copeland, N.G.; Gilbert, D.J.; Jenkins, N.A.; Bacon, K.B.; et al. TECK: A novel CC chemokine specifically expressed by thymic dendritic cells and potentially involved in T cell development. *Immunity* **1997**, *7*, 291. [[CrossRef](#)]
83. Wurbel, M.-A.; Philippe, J.M.; Nguyen, C.; Victorero, G.; Freeman, T.; Wooding, P.; Miazek, A.; Mattei, M.G.; Malissen, M.; Jordan, B.R.; et al. The chemokine TECK is expressed by thymic and intestinal epithelial cells and attracts double- and single-positive thymocytes expressing the TECK receptor CCR9. *Eur. J. Immunol.* **2000**, *30*, 262. [[CrossRef](#)] [[PubMed](#)]
84. Svensson, M.; Agace, W.W. Role of CCL25/CCR9 in immune homeostasis and disease. *Expert Rev. Clin. Immunol.* **2006**, *5*, 759–773. [[CrossRef](#)]
85. Eksteen, B.; Grant, A.J.; Miles, A.; Curbishley, S.M.; Lalor, P.F.; Hübscher, S.G.; Briskin, M.; Salmon, M.; Adams, D.H. Hepatic endothelial CCL25 mediates the recruitment of CCR9+ gut-homing lymphocytes to the liver in primary sclerosing cholangitis. *J. Exp. Med.* **2004**, *200*, 1511–1517. [[CrossRef](#)] [[PubMed](#)]
86. Jeyaseelan, S.; Chu, H.W.; Young, S.K.; Worthen, G.S. Transcriptional profiling of lipopolysaccharide-induced acute lung injury. *Infect Immun.* **2004**, *72*, 7247–7256. [[CrossRef](#)] [[PubMed](#)]
87. Mahler, J.F.; Stokes, W.; Mann, P.C.; Takaoka, M.; Maronpot, R.R. Spontaneous lesions in aging FVB/N mice. *Toxicol. Pathol.* **1996**, *24*, 710–716. [[CrossRef](#)] [[PubMed](#)]
88. Jhamat, N.; Niazi, A.; Guo, Y.; Chanrot, M.; Ivanova, E.; Kelsey, G.; Bongcam-Rudloff, E.; Andersson, G.; Humblot, P. LPS-treatment of bovine endometrial epithelial cells causes differential DNA methylation of genes associated with inflammation and endometrial function. *BMC Genom.* **2020**, *21*, 385. [[CrossRef](#)] [[PubMed](#)]
89. Chen, J.; Wu, Y.; Sun, Y.; Dong, X.; Wang, Z.; Zhang, Z.; Xiao, Y.; Dong, G. Bacterial lipopolysaccharide induced alterations of Genome-Wide DNA methylation and promoter methylation of lactation-related genes in bovine mammary epithelial cells. *Toxins* **2019**, *1*, 298. [[CrossRef](#)]

**Disclaimer/Publisher’s Note:** The statements, opinions and data contained in all publications are solely those of the individual author(s) and contributor(s) and not of MDPI and/or the editor(s). MDPI and/or the editor(s) disclaim responsibility for any injury to people or property resulting from any ideas, methods, instructions or products referred to in the content.